PHYSICAL REVIEW B VOLUME 42, NUMBER 14 15 NOVEMBER 1990-I

# Optical properties of polycrystalline nickel silicides

M.Amiotti and A.Borghesi
*Dipartimento di Fisica "A.Volta," Università degli Studi di Pavia, I-27100 Pavia, Italy*

G.Guizzetti and F.Nava
*Dipartimento di Fisica, Università degli Studi di Modena, I-41100 Modena, Italy*
(Received 1 June 1990)

The near-normal reflectivity of polycrystalline $Ni_3Si$, $Ni_2Si$, NiSi, and $NiSi_2$ from 0.01 to 6 eV and the dielectric functions obtained by Kramers-Kronig analysis are presented. The effect of an oxide overlayer on the optical properties is also considered. The low-energy response is discussed in terms of the Drude model and compared with the transport measurements. The higher-energy interband spectrum is interpreted on the basis of the calculated density of states and photoemission results. In particular, the optical structures of $NiSi_2$ are correlated to interband transitions using the joint density of states obtained by band-structure calculations.

## I. INTRODUCTION

The widespread use of thin films in microelectronic and optical devices has stimulated great interest in detailed understanding of their growth, as well as electrical and optical properties. In the past few years, thin films of transition-metal silicides have gained particular interest in solid state technology as they permit both Ohmic and Schottky-barrier contacts in very-large-scale integration. Investigations have therefore mainly focused on the effect of material preparation on the resistivity and the properties of the Si-silicide interface, in relation to the Schottky barrier problem.[1-4] Comparatively few systematic studies have been devoted to the optical properties of the silicides.[5-7]

Silicides are used to form a layer on the top of poly-Si gate material (polycide), enhancing the interconnection capability by reducing the resistance. Silicides produced from the near noble metals Ni, Pt and Pd are particularly used because they form metal-rich silicides at relatively low temperature[8] with respect to other silicides.[9] Recently, high-quality homoepitaxial films of $NiSi_2$ have been grown by molecular-beam epitaxy on (100) and (110) Si at room temperature[10] and (111) silicon,[11] providing additional flexibility for many device applications as well as the opportunity to study metal-semiconductor interfaces, in particular, the effect of $NiSi_2$ orientation on the Schottky-barrier height.[11,12] Moreover Ni silicides are used in Schottky-barrier infrared detectors, making the study of their optical properties even more interesting.

Various experimental studies have been carried out on Ni silicides, concerning phase diagrams[8], electrical resistivity and Hall coefficient,[13-15] sheet resistance,[16] structure and morphology by Rutherford-backscattering spectrometry and x-ray diffraction,[17] TEM analysis,[18] surface-extended x-ray-absorption fine structure[19] and low-energy electron diffraction.[20] Electronic structure has been investigated by photoemission,[21-26] x-ray photoemission,[27-29] inverse photoemission,[30] energy-loss spectroscopy,[31] photoabsorption,[32] and Auger-electron spectroscopy.[20,33,34]

Some reports regard the optical properties of Ni silicides. Henrion et al.[35] measured the reflectivity of Ni and NiSi from 0.05 to 4 eV. Humbert and Cros[36] performed a comparative study of the reflectivity of Ni and its silicides ($Ni_4Si$, $Ni_2Si$, NiSi, $NiSi_2$) in the range 0.6–4 eV. Chen and Lue[37] obtained the refractive index $n$ and the extinction coefficient $k$ of $Ni_2Si$, NiSi, $NiSi_2$ with ellipsometry in the 400 to 700 nm wavelength interval. Jimenez *et al.*[38] used ellipsometry to measure the dielectric functions of epitaxial films of $NiSi_2$ from 0.9 to 4 eV.

In this paper we present a systematic study on the reflectivity of Ni, $Ni_3Si$, $Ni_2Si$, NiSi, $NiSi_2$, measured with high precision on a more extended spectral range (0.01–6 eV). The optical functions $n$, $k$, $\epsilon_1$, and $\epsilon_2$ by a Kramers-Kronig (KK) analysis could therefore be derived and checked through ellipsometric measurements at one selected wavelength. We also consider the effect of an amorphous $SiO_2$ overlayer on the optical response. The spectra are analyzed in terms of intraband and interband transitions by using the calculated electronic band structures[21,39-41] and density of states (DOS).[23,42,43] We fit $\epsilon_1$ and $\epsilon_2$ far-infrared (FIR) spectra with a Drude-like model, obtaining both the free-carriers plasma frequency $\omega_p^2$ and the scattering time $\tau$, which are then compared with results from transport measurements.

## II. EXPERIMENTAL PROCEDURE AND RESULTS

The samples were prepared by electron-beam evaporation onto oxidized silicon wafers held at room temperature. Amorphous silicon films and nickel films were evap-

 ©1990 The American Physical Society

orated consecutively at a pressure below 4x10$^{-7}$ Torr. The thickness ratios of silicon to nickel were selected in order to produce the correct stoichiometry in the silicides. The four ratios of thicknesses (in Å) were 1500/500, 1890/940, 1350/1270, and 680/1300. They correspond to the following Ni-to-Si atomic ratios: 3:1, 2:1, 1:1, and 1:2, respectively. Rutherford backscattering spectroscopy with 2 MeV $^4He^+$ ion beam was used for depth composition analysis and to determine compound thicknesses, assuming bulk density values for Si and Ni and tabulated scattering cross sections. Thicknesses of 1900, 2200, 1900, and 2000 Å were obtained for $Ni_3Si$, $Ni_2Si$, NiSi, and $NiSi_2$, respectively, after thermal annealing at 850 °C for 1 h. Particular care was taken during the furnace annealing in order to reduce the intake of impurities; the details of the aforementioned process have been described elsewhere[6].

The surface of the $SiO_2$ layer before the deposition did not show features or roughness under scanning electron microscopy (SEM). Surface morphology for both the as-deposited and fully annealed thin films was also examined by SEM. The surfaces resulted extremely smooth in both cases, exhibiting features and roughness comparable to the underlying $SiO_2$.

The phases and the crystalline structures were identified by glancing incidence x-ray diffraction in a Bragg-Brentano reflection goniometer with scintillation counter and in a Wallace-Ward cylindrical texture camera with photographic recorder.

The dc electrical resistivity ($\rho_{dc}$) and Hall voltage were measured at room temperature on annealed samples in which the reaction was completely finished. Thin copper wires were indium soldered to the four contact pads of a Van der Pauw pattern, obtained by deposition of Ni and Si through a metallic mask. The $\rho_{dc}$ values at room temperature and the Hall coefficient, $R_H$, are reported in Table I, together with the apparent charge carrier density $N$ inferred from the Hall coefficient. We note that both $\rho_{dc}$ and $N$ values reasonably agree with those previously reported:[13-15] in particular, the positive sign of $R_H$ in $Ni_2Si$ and $NiSi_2$ indicate that two carrier species are present and that holes are the dominant species at room temperature. This can be ascribed to the complicated and anisotropic band structures of the compounds. In such a case the Hall constant is, in fact, determined by the difference in the number of electrons (occupied states) and the number of holes (empty states) at the Fermi surface. This model has been invoked to explain the anisotropic behavior of the resistivity observed in $MoSi_2$ single crystal.[44]

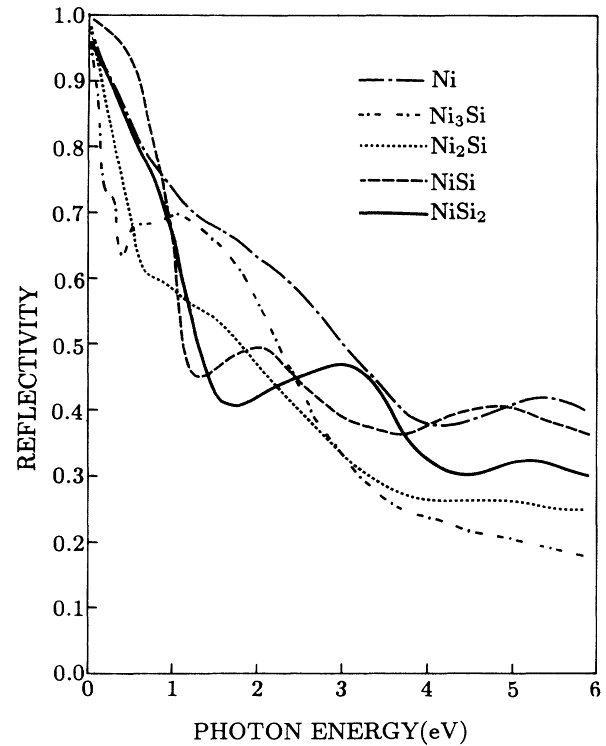

FIG. 1. Room-temperature reflectivity ($R$) of $Ni_3Si$, $Ni_2Si$, NiSi, $NiSi_2$, and pure Ni.

Reflectivity ($R$) at near-normal incidence and at room temperature was measured in the 0.5–6 eV photon-energy range using an Al mirror as reference and a reflectometer mounted on a Perkin Elmer 330 automatic spectrophotometer. From 0.01 to 0.5 eV $R$ was measured by a Fourier-transform spectrometer Bruker IFS 113v, using a Au mirror as reference. The $R$ values from the two spectrometers in the overlapping spectral range agreed within the limits of experimental uncertainty (±1%). As pointed out in Refs. 36 and 45, a superficial $SiO_2$ layer (20–40 Å) transparent in the visible and uv is present because the samples were exposed to air. Generally, the $R$ spectrum, and consequently the dielectric function, are influenced by surface roughness, particularly in the uv range. However the very flat and uniform surface of our samples, as shown by SEM measurements, produced negligible light diffusion .

The $R$ spectra of $Ni_3Si$, $Ni_2Si$, NiSi, and $NiSi_2$ from 0.01 to 6 eV are shown in Fig. 1 and compared to that

TABLE I. The experimental values of optical ($\omega_p, \tau, \rho_{opt}$) and electrical ($\rho_{dc}, R_H, N$) parameters at room temperature for Ni silicides.

| | $\omega_p$ (eV) | $\tau$ ($10^{-15}$ sec) | $\rho_{opt}$ ($\mu\Omega$ cm) | $\rho_{dc}$ ($\mu\Omega$ cm) | $R_H$ ($10^{-4}$ cm$^3$ C$^{-1}$) | $N$ ($10^{21}$ cm$^{-3}$) |
|---|---|---|---|---|---|---|
| $Ni_3Si$ | 3.4 | 14.0 | 96 | 94 | -9.5 | $6e^-$ |
| $Ni_2Si$ | 2.4 | 15.3 | 55 | 25 | 1.2 | $50e^+$ |
| NiSi | 3.8 | 18.8 | 18.5 | 12 | -1.3 | $48e^-$ |
| $NiSi_2$ | 4.6 | 4.4 | 55 | 34 | 3.2 | $19e^+$ |

of pure Ni. The high reflectivity for all silicides in the infrared region is typical of the noble metals: it displays a broad shoulder followed by a sharp cutoff , which systematically shifts toward higher energies as the Si content increases. The main peak in $R$, due to interband transitions, displays the same behavior. This feature is absent in the pure Ni as well as in other quasinoble or transition metals, where $R$ falls off quasimonotonically from the FIR. We note that the measurements over a large spectral range, beginning from FIR, indicate a continous evolution of the Ni silicides spectral shape, with no difference between Ni and Si rich compounds, stated in Ref. 36. We can compare our optical spectra with those previously reported (all, except the Ni case, are relative to a narrower spectral range) keeping in mind that some disagreement about the actual magnitude of optical structures may depend on sample preparation, accuracy of the optical measurements, and the method by which the experimental data are analyzed. The structure energies, instead, agree in almost every case. The reflectivity of Ni from Lynch *et al.*[46] is in excellent agreement with our spectrum above 1 eV, while is little higher in ir and FIR where, due to the difficulty of a precise and direct measure, it was derived from absorbance ($A = 1 - R$), measured at 4 K by calorimetric technique. The reflectance of Henrion *et al.*,[35] in the Ni case is higher than ours in uv, while in the NiSi is lower over the entire spectral range. The $R$ spectra of Humbert and Cros[36] for both Ni and silicides agree qualitatively with ours, but are systematically higher (this could be ascribed to the use of a faulty mirror as reference). As regards the reflectivity derived from ellipsometry, the spectra of Jimenez *et al.*[38] agree qualitatively with ours, being 10% higher in uv, while the results of Cheng and Lue[37] disagree totally with ours and those in the literature.

To provide a more complete description of the optical properties we performed a KK analysis of the reflectivity, yielding the complex dielectric function $\tilde{\epsilon}(\omega) = \epsilon_1(\omega) + i\epsilon_2(\omega)$ and the complex refraction index $\tilde{n}(\omega) = n(\omega) + ik(\omega)$, plotted in Figs. 2 to 5. We extrapolated the $R$ spectrum beyond the highest experimental energy $\omega_o$ with a tail $R(\omega) = R(\omega_0)\ (\omega_0/\omega)^s$. The $s$ value was determined so that the $n$ and $k$ values from KK agreed with the experimental values at $\omega$=1.96 eV, directly measured with a Sopra MOSS-ES4G ellipsometer. The corresponding $R$ values obtained using the ellipsome-

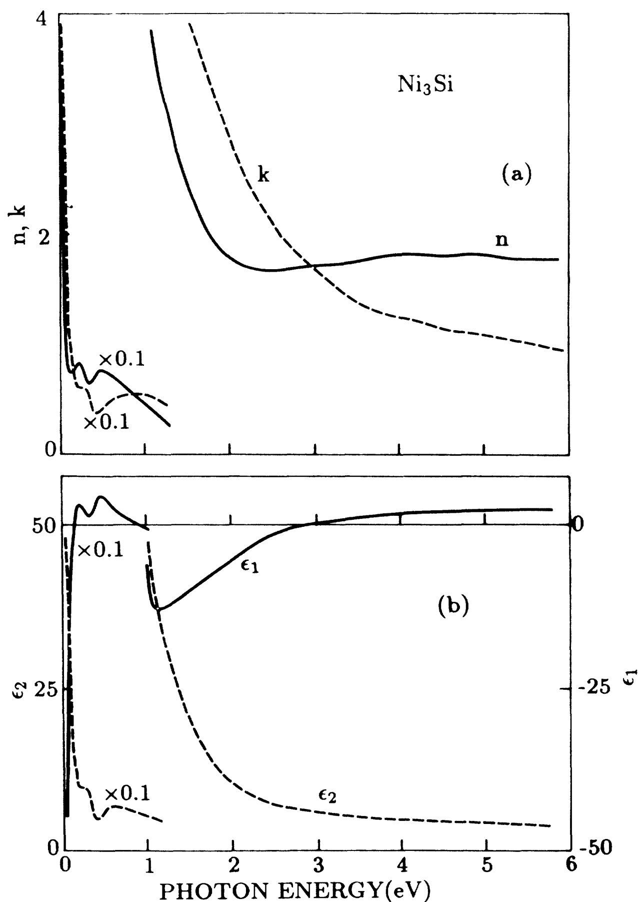


FIG. 2. (a) Real ($\epsilon_1$) and imaginary ($\epsilon_2$) parts of the dielectric function of $Ni_3Si$. (b) Refractive index ($n$) and extinction coefficient ($k$) of $Ni_3Si$.

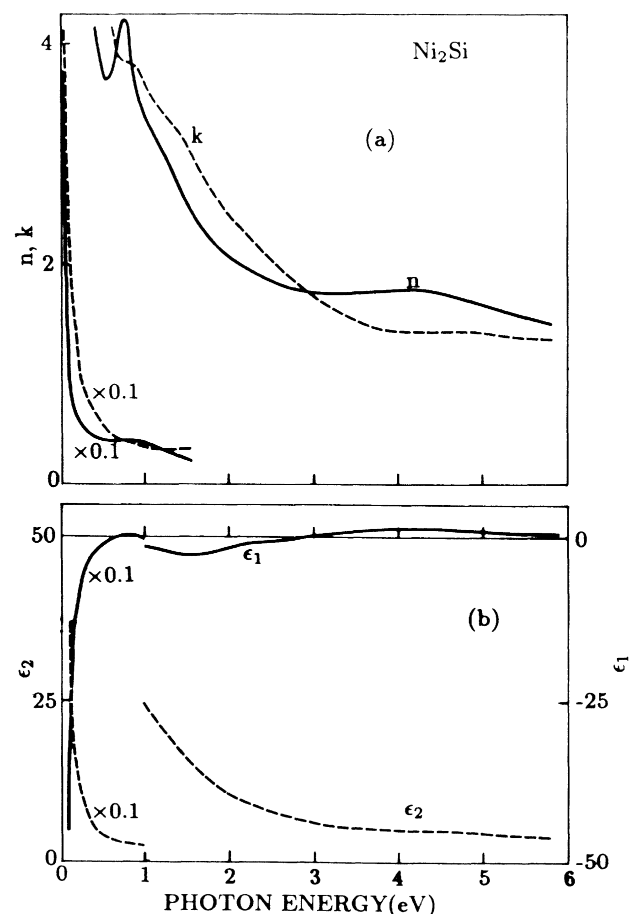


FIG. 3. (a) Real ($\epsilon_1$) and imaginary ($\epsilon_2$) parts of the dielectric function of $Ni_2Si$. (b) Refractive index ($n$) and extinction coefficient ($k$) of $Ni_2Si$.

ter and the spectrophotometer coincide within the limits of experimental uncertainty. We obtained $s \approx 2$ for all the compounds examined. We note that it did not correspond to the constraint $s=4$ used, for example, in Pt silicides.[47] This is not surprising, because it is well known[48] that an inverse fourth law does not work up to energies much higher than in our spectra, even for pure transition metals. The behavior of $\epsilon_1$ and $\epsilon_2$ in ir is that expected for free-carrier intraband transitions: $\epsilon_1$ is negative and increases with energy, crossing the zero axis at what is called the screened plasma frequency, while $\epsilon_2$ decreases with energy. The screening effect, which lowers the plasma energy, is due to interband transitions, which partially are superimposed on intraband transitions. At higher energies, where intraband contribution is exhausted, $\epsilon_2$ is quasiflat in Ni-rich silicides while it shows some weak structures in Si-rich silicides, which correspond to much stronger structures in $R$ spectrum. This occurs because the great oscillator strength of previous transitions exhausts the sum rule and forces $\epsilon_2$ to assume lower values in this energy range.

The effect of oxides on the optical spectra in the visible-uv region has been estimated by employing a three-phase model: $NiSi_2$ (substrate)–amorphous $SiO_2$ film–ambient. In the limit of a film thickness $d \ll \lambda$, the following expression for the pseudodielectric function $< \bar{\epsilon} >$ is obtained:[49]

$$< \bar{\epsilon} > \simeq \bar{\epsilon}_s + \frac{4\pi i d}{\lambda} \frac{\bar{\epsilon}_s(\bar{\epsilon}_s - \bar{\epsilon}_{\rm ox})(\bar{\epsilon}_{\rm ox} - \bar{\epsilon}_a)}{\bar{\epsilon}_{\rm ox}(\bar{\epsilon}_s - \bar{\epsilon}_a)\left(\bar{\epsilon}_s - \bar{\epsilon}_a \sin^2\phi\right)^{1/2}}. \quad (1)$$

Here $\phi$ is the angle of incidence, and $\bar{\epsilon}_s$, $\bar{\epsilon}_{\rm ox}$, and $\bar{\epsilon}_a$ are the effective complex dielectric functions of the substrate, of the amorphous oxide and of the ambient, respectively. In our case $< \bar{\epsilon} >$ is the complex dielectric function as given by the KK analysis, $\bar{\epsilon}_a = 1$, $\sin\phi \approx 0$, and $\bar{\epsilon}_{\rm ox}$ values for amorphous $SiO_2$ are kept from Ref. 50. Using different values of $d$ we obtained the effective dielectric functions of $NiSi_2$, which is shown in Fig. 6 for two $d$ values (10 and 50 Å). As expected, the oxide does not introduce new structures because amorphous $SiO_2$ is transparent in the interval examined, but it appreciably affects $< \bar{\epsilon} >$, for $d \geq 50$ Å.

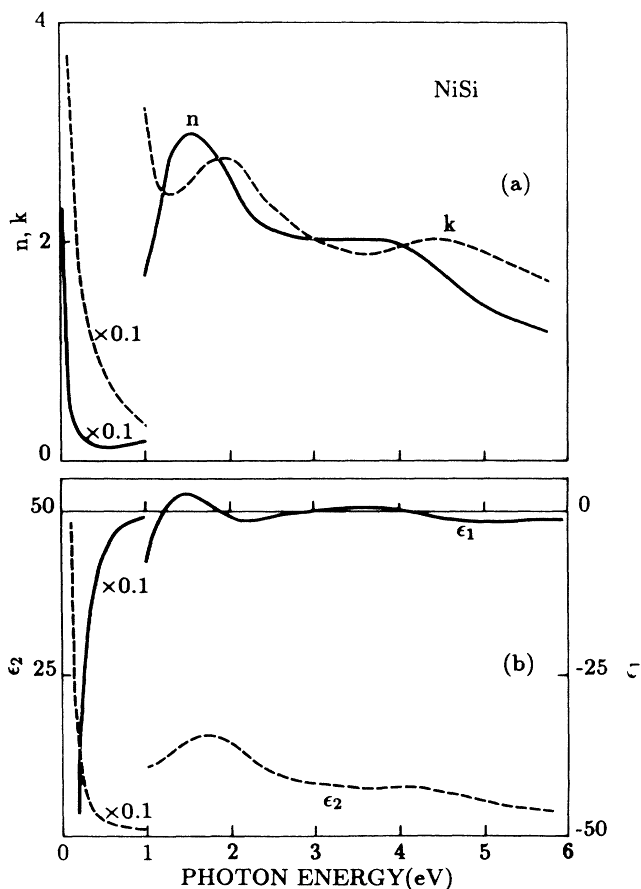


FIG. 4. (a) Real ($\epsilon_1$) and imaginary ($\epsilon_2$) parts of the dielectric function of NiSi. (b) Refractive index ($n$) and extinction coefficient ($k$) of NiSi.

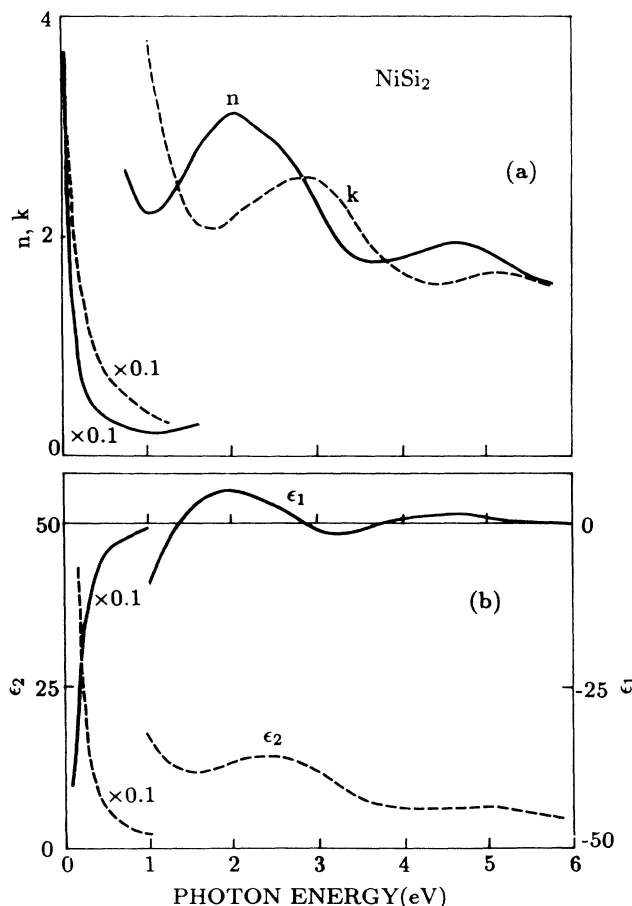


FIG. 5. (a) Real ($\epsilon_1$) and imaginary ($\epsilon_2$) parts of the dielectric function of $NiSi_2$. (b) Refractive index ($n$) and extinction coefficient ($k$) of $NiSi_2$.

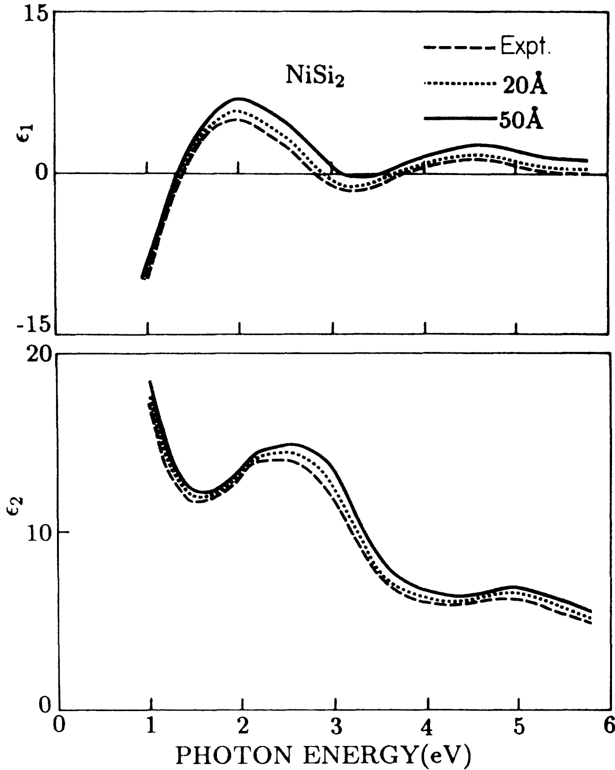


FIG. 6. Effective dielectric functions of $NiSi_2$ obtained from pseudodielectric function (dashed line) for two different thicknesses of $SiO_2$ surface layer.

## III. DISCUSSION

The knowledge of the electronic band structure, the related joint density of states (JDOS), and oscillator strengths is fundamental for an accurate interpretation of the optical spectra. To our knowledge no JDOS has been calculated for transition-metal silicides. Most of the theoretical studies concern the role of silicon ($s$ and $p$) and metal ($d$) states in bonding and the calculation of the DOS. The latter permits direct comparison with many x-ray and uv photoemission and inverse photoemission experimental results. This is also true for Ni silicides. In particular $NiSi_2$ has been extensively studied, both theoretically and experimentally, due to the vivid discussion of its Schottky barrier and the stability of its crystalline structure.

So we will qualitatively discuss some general trends in our spectra on the basis of the DOS and the chemical bonding properties. A more detailed analysis will be devoted to $NiSi_2$, where several band structure calculations allow some assignment of the observed optical structures.

Some controversies still exist concerning the details of bonding (charge transfer and ionic contribution to the bond, and electronic configuration in equilibrium). However the different calculations on Ni silicides are in good overall quantitative agreement with experimental results and yield very similar DOS, with the following main features.

(a) The chemical bond is essentially due to the coupling between Si-3$p$ and Ni-3$d$ states, which produces bonding and antibonding $p$-$d$ features below and above the Fermi level $E_F$, respectively, separated by a nonbonding (purely $d$) region near $E_F$.

(b) Going from the Ni-rich ($Ni_3Si$) to Si-rich ($NiSi_2$) silicides, the Ni-Ni nearest-neighbor distance increases by more than 50%. The decreasing Ni-Ni interaction produces narrower and sharper nonbonding $d$-bands, with a peak position shifting toward higher binding energy (1.2, 1.3, 1.8, and 3.2 eV below $E_F$ for $Ni_3Si$, $Ni_2Si$, NiSi, and $NiSi_2$ respectively).[42,43]

(c) In the Ni-rich silicides the Fermi surface has a relevant $d$ character, while in $NiSi_2$ it has a $p$-$d$ antibonding character (extending 2 eV under $E_F$), approximately corresponding to one $p$ and one $d$ electron per atom.

(d) The binding energy of the Ni-3$p$ core level varies with Si content almost identically to the $d$-band peak, while the binding energy of Si-2$p$ levels does not change appreciably. The Si-3$s$ states are not involved in the bond, forming an empty band under antibonding bands.

On the basis of this preliminary information, we analyzed our optical results by distinguishing two different contributions typical of a metal spectrum: the intraband, due to the free electrons, and the interband transitions. However, we must recall that in pure Ni it is already impossible to clearly separate the two contributions even at rather low energies. In fact theoretical calculations predict the presence of interband transition around 0.25 eV, as a consequence of the intersection of the $d$-band complex with the Fermi level. The conductivity spectra, deduced from absorptivity measured at 4 K by a calorimetric technique, and the thermoreflectance spectra show a peak at 0.28 and 0.25 eV, respectively.[46] The data satisfy a Drude-like expression only below 0.13 eV.

In the Ni silicides, the sharp cutoff in $R$ followed by a peak at higher energies only roughly separates the intraband from the interband regions. This peak can be associated to the strong interband transitions from nonbonding states below $E_F$ to antibonding states above $E_F$. In fact a strong correlation exists between the positions of the peaks in $R$ (approximately 0.9, 1.1, 2, and 3.1 eV going from the $Ni_3Si$ to $NiSi_2$) and the peaks of DOS [point (b)] and of photoemission spectra.[22] However the presence of some shoulders in the dielectric functions and the band calculations for $NiSi_2$ indicate that interband transitions can also occur at energies lower than the $R$ cutoff (or the zero crossing in $\epsilon_1$). They are superimposed on the free-carrier intraband transitions, causing $\tilde{\epsilon}$ to differ from the Drude formula:

$$\tilde{\epsilon}(\omega) = \epsilon_\infty - \frac{\omega_p^2}{\omega(\omega + i/\tau)}. \tag{2}$$

Here $\epsilon_\infty$ is the high-frequency dielectric constant, $\omega_p$ and $\tau$ the plasma frequency and the relaxation time of the free carriers, respectively. The pair of the parameters $\omega_p$ and $\tau$ are constrained by the conductivity $\sigma(\omega) = \omega\epsilon_2(\omega)$ at zero frequency: $\sigma(0) = \omega_p^2\tau/4\pi$. When interband tran-

sitions contribute, we do not have free-carrier resonance but rather hybrid resonance resulting from the cooperative behavior of both free and bound carriers. Alternatively this resonance may be described as due to the free carriers screened by a frequency-dependent dielectric constant $\bar{\epsilon}_{\rm inter}(\omega)$, which replaces $\epsilon_\infty$ in Eq.(2).

We tested the applicability of the Drude model by plotting $\epsilon_1(\omega)$ versus $\omega\epsilon_2(\omega)$, which should give a straight line. For all Ni silicides we find a constant slope only for energies lower than about 0.3 eV. The plot for $NiSi_2$ is shown in Fig. 7, as an example. Correspondingly the plots of $1/\omega\epsilon_2(\omega)$ and of $1/|\epsilon_1(\omega)|$ versus $\omega^2$ show linearity, according to Eq.(2), with slope $\tau/\omega_p^2$ and $1/\omega_p^2$, respectively. The values $\omega_p$ and $\tau$ obtained from a best fit are reported in Table I, together with the optical resistivity [$\rho_{\rm opt} = 1/\sigma(0)$]. We note that, apart from systematically higher values of $\rho_{\rm opt}$ with respect to $\rho_{\rm dc}$, the trend in the function of Si content is quite satisfactory. In particular, the value of $\omega_p$ for $NiSi_2$ is lower than the value ranging from 6.5 to 7.5 eV, quoted in Ref. 38. The difference is due to the fact that in Ref. 38 a value of $\rho_{\rm dc}$=34 $\mu\Omega$ cm is used to derive $\omega_p$ from $\epsilon_2$ ellipsometric measurements near the hybrid plasma resonance. This value of $\rho_{\rm dc}$ is coincident with our measurements, but is about one-half of the $\rho_{\rm opt}$ value, self-consistently derived from optical measurements in the FIR. Using $\omega_p^2 = 4N\pi e^2/m^*$ as the plasma frequency we obtained the effective-mass values $m^*$, which in unity of $m_e$ are 6, 4, 1.24 for $Ni_2Si$, NiSi, and $NiSi_2$ respectively. This decrease with increasing Si content is consistent with the results summarized in points (b) and (c), i.e., the metallic character predominantly results from *d* electrons in Ni rich silicides, but also from *s*- and *p*-like free electrons in $NiSi_2$. It is interesting to compare these values of $m^*$ with those obtained from $\rho_{\rm dc}$ versus $T$ curves.[51] In fact the electron-phonon coupling constant $\lambda$ is proportional to the resistivity slope $a_\infty$ at $T \gg \theta$ ($\theta$ is the Debye temperature) through the relation:[52]

$$\lambda = 0.246\, \omega_p^2\, a_\infty . \tag{3}$$

Taking $a_\infty$ from a best fit of experimental curves, $N$ from Table I, and assuming $\lambda$=0.25, we find $m^*$=4.5 $m_e$ for NiSi and $m^*$=1.4 $m_e$ for $NiSi_2$. The evaluation of $m^*$ for $NiSi_3$ is not possible due to the strong dependence[51] of $R_H$ on $T$, which suggests the presence of complex multicarrier effects and makes unreliable the $N$ value. Morever $\rho_{\rm dc}$ versus $T$ curve shows that a classical transport model is inapplicable already at room temperature.

In the case of $NiSi_2$ we calculated the intraband contribution $\epsilon_{2\rm intra}$ from Eq.(2) with the parameters reported in Table I, assuming $\tau$ to be constant over the entire range. The results are compared in Fig. 8 with $\epsilon_2$ total and with $\epsilon_{2\rm inter} = \epsilon_2 - \epsilon_{2\rm intra}$, showing that the interband transition edge is at 0.3 eV.

We compare the interband optical response of $NiSi_2$ with the calculated band structure [39] and the relative joint density of states (JDOS), which has been graphically derived in Ref. 53, along high-symmetry directions of the Brillouin zone, taking into account the selection rules. We recall that $NiSi_2$ crystallizes in the fluoride structure, i.e., it has a fcc lattice with $a$ = 5.4 Å and with a molecular formula per unit cell. The Si atoms form a simple cubic sublattice with Ni atoms occupying

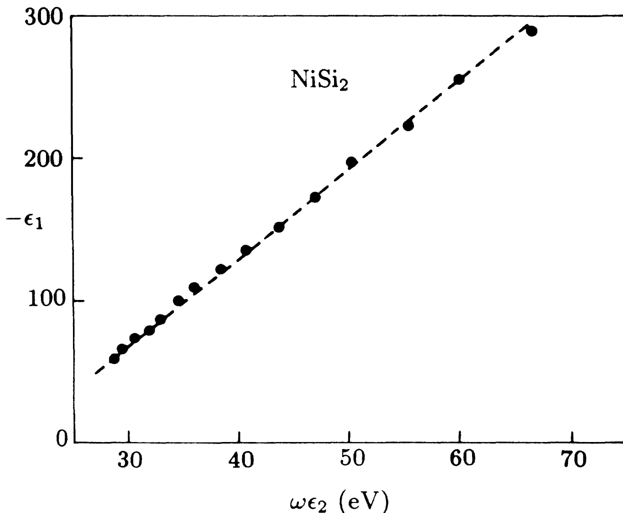


FIG. 7. $\epsilon_1$ versus $\omega\epsilon_2$ plot for $NiSi_2$.

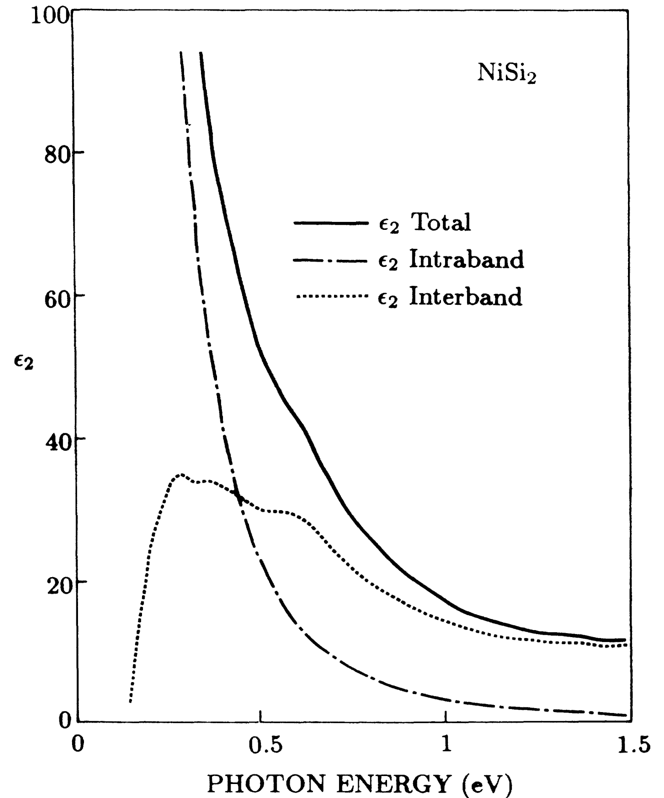


FIG. 8. $\epsilon_2$ spectrum of $NiSi_2$ showing the intraband and interband contributions.

the center of every other cube. Each Si atom is therefore tetrahedrally surrounded by 4 Ni atoms, at a distance of 2.34 Å while each Ni is surrounded by 8 Si on the cube corners.

The band structure near the Fermi level is displayed in Fig. 9. It was calculated[39] using a self-consistent linear combination of Gaussian orbitals, with a basis set consisting of all atomic orbitals up to Si $3p$ and Ni $4p$, plus two $p$ and $d$ and three $s$ Gaussian orbitals on each atomic site. Reference 53 verified that another band calculation, based on the augmented plane-wave method,[21] yields the same results, at least concerning the low-energy interband transitions.

The selection rules and the JDOS calculated in Ref. 53 show that the transitions $\Sigma_3 \rightarrow \Sigma_1$ near the $\Gamma$ point and $\Sigma_4 \rightarrow \Sigma_1$ (dashed area in Fig. 9) are responsible for a peak at $\sim 2$ eV in the JDOS, while the structure at 3.2 eV is due to transitions $Q_2 \rightarrow Q_1$ and $Q_2 \rightarrow Q_2$ around $L$ point. These peaks correspond well to the large structure centered at $\sim 2.5$ eV in the $\epsilon_2$ experimental spectrum. Moreover the transitions $\Delta_3 \rightarrow \Delta_1$ at lower energies (beginning at $\sim 0.3$ eV and extending up to $\sim 1$ eV) are allowed, which connect antibonding states Ni($d$)-Si($s,p$) below and above the $E_F$. These transitions determine the structures observed in the $\epsilon_{2\text{inter}}$ spectrum (Fig. 8) with the edge at 0.3 eV, and are responsible for the screening of the free-carrier plasma resonance and for the gradual fall of the reflectivity in ir. Finally the small structure in $\epsilon_2$ at high energy ($\sim 5$ eV) may be ascribed to $X_1 \rightarrow X_1$ or $\Delta_1 \rightarrow \Delta_1$ transitions .

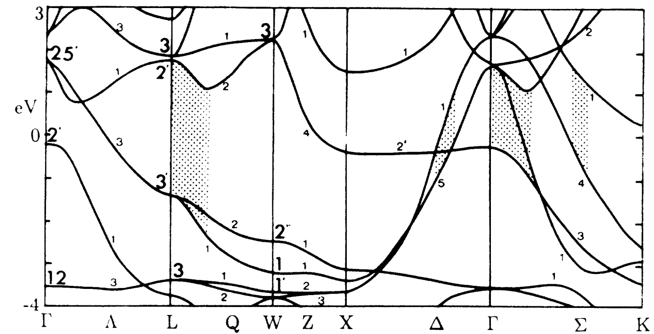


FIG. 9. Energy bands near the Fermi level for $NiSi_2$ (from Bylander *et al.*, Ref. 39). The dashed areas represent allowed transitions determining structures in the joint density of states.

## ACKNOWLEDGMENTS

We wish to thank M.Moscardini for technical aid. This work was partially supported by Progetto Finalizzato "Materiali e Dispositivi per Elettronica a Stato Solido (MADESS)" and by Gruppo Nazionale Struttura della Materia del Consiglio Nazionale delle Ricerche, Italy.

[1] F. Nava, K. N. Tu, E. Mazzega, M. Michelini, and G. Queirolo, J. Appl. Phys. **61**, 1085 (1987).
[2] J. C. Hensel, R. T. Tung, J. M. Poate, and F. C. Unterwald, Appl. Phys. Lett. **44**, 913 (1984).
[3] J. C. Hensel, R. T. Tung, J. M. Poate, and F. C. Unterwald, Phys. Rev. Lett. **54**, 1840 (1985).
[4] *Surfaces and Interfaces: Physics and Electronics*, edited by R. S. Bauer (North-Holland, Amsterdam, 1982), and references therein.
[5] A. Borghesi, L. Nosenzo, A. Piaggi, G. Guizzetti, C. Nobili, and G. Ottaviani, Phys. Rev. B **38**, 10 937 (1988).
[6] A. Borghesi, A. Piaggi, G. Guizzetti, F. Nava, and M. Bacchetta, Phys. Rev. B **40**, 3249 (1989).
[7] A. Borghesi, A. Piaggi, G. Guizzetti, F. Lèvy, M. Tanaka, and H. Fukutani, Phys. Rev. B **40**, 1611 (1989).
[8] C. Canali, G. Majni, G. Ottaviani, and G. Celotti, J. Appl. Phys. **50**, 255 (1979).
[9] E. G. Colgan, B. Y. Tsaur, and J. M. Mayer, Appl. Phys. Lett. **37**, 938 (1980).
[10] R. T. Tung, F. Schrey, and S. M. Yalisove, Appl. Phys. Lett. **55**, 2005 (1989).
[11] M. Ospelt, J. Henz, L. Flepp, and H. Von Känel, Appl. Phys. Lett. **52**, 227 (1988).
[12] A. Kikuchi, Phys. Rev. B **40**, 8024 (1989).
[13] K. Pomoni, and C. Krontiras, J. Phys. D **21**, 780 (1988).
[14] J. C. Hensel, R. T. Tung, J. M. Poate, and F. C. Unterwald, in *Proceedings of the 17th International Conference on the Physics of Semiconductors*, edited by J. D. Chadi and W. A. Harrison (Springer, New York, 1985), p.197.
[15] E.G. Colgan, M. Maenpaa, M. Finetti, and M. A. Nicolet, J. Electron. Mater. **12**, 413 (1983).
[16] A. Singh, and W. S. Khokle, Phys. Status Solidi A **100**, K25 (1987).
[17] F. d'Heurle, C. S. Peterson, J. E. E. Baglin, S. J. La Placa, and Y. Wong, J. Appl. Phys. **55**, 4208 (1984).
[18] H. Föll, P. S. Ho, and K. N. Tu, Philos. Mag. A **45**, 31 (1982).
[19] F. Comin, J. E. Rowe, and P. H. Citrin, Phys. Rev. Lett. **51**, 2402 (1983).
[20] W. S. Yang, F. Jona, and P. M. Marcus, Phys. Rev. B **28**, 7377 (1983).
[21] Y. J. Chabal, D. R. Hamann, J. E. Rowe, and M. Schlüter, Phys. Rev. B **25**, 7598 (1982).
[22] A. Franciosi, J. H. Weaver, and F. A. Schmidt, Phys. Rev. B **26**, 546 (1982).
[23] Y. Shiraki, K. L. I. Kobayashi, H. Daimon, A. Ishizuka, S. Sugaki, and Y. Murata, Physica **117&118**, 843 (1983).
[24] J. H. Weaver, A. Franciosi, and V. L. Moruzzi, Phys. Rev. B **29**, 3293 (1984).
[25] O.Bisi, C. Calandra, U. Del Pennino, P. Sassaroli, and S. Valeri, Phys. Rev. B **30**, 5696 (1984).
[26] H. Hinkel, L. Sorba, H. Haak, K. Horn, and W. Braun, Appl. Phys. Lett. **50**, 1257 (1987).
[27] P. J. Grunthaner, F. J. Grunthaner, and J. W. Mayer, J. Vac. Sci. Technol. **17**, 924 (1980).
[28] N. W. Cheung, P. J. Grunthaner, J. W. Mayer, and B. M. Ullrich, J. Vac. Sci. Technol. **18**, 917 (1981).
[29] P. J. Grunthaner, F. J. Grunthaner, and A. Madhukar,

Physica **117&118**, 831 (1983).
[30] M. Azizan, R. Baptist, G. Chauvet, and T. A. Nguyen, Solid State Commun. **57**, 1 (1986).
[31] U. Del Pennino, C. Mariani, S. Valeri, G. Ottaviani, M. G. Betti, S. Nannarone, and M. De Crescenzi, Phys. Rev. B **34**, 2875 (1986).
[32] M. G. Betti, U. Del Pennino, C. Mariani, A. M. Fiorello, M. Pedio, S. Perugini, and S. Nannarone (private communication).
[33] U. Del Pennino, P. Sassaroli, S. Valeri, G. M. Bertoni, O. Bisi, and C. Calandra, J. Phys. C **16**, 6309 (1983).
[34] S. Valeri, U. Del Pennino, P. Sassaroli, and G. Ottaviani, Phys. Rev. B **28**, 4277 (1983).
[35] W. Henrion, and H. Lange, Phys. Status Solidi B **112**, K57 (1982).
[36] A. Humbert and A. Cros, J. Phys. Lett. **44**, L929 (1983).
[37] H. W. Cheng, and J. T. Lue, J. Appl. Phys. **59**, 2165 (1986).
[38] J. R. Jimenez, Z. C. Wu, L. J. Schowalter, B. D. Hunt, R. W. Fathauer, P. J. Grunthaner, and T. L. Lin, J. Appl. Phys. **66**, 2738 (1989).
[39] D. M. Bylander, L. Kleinman, K. Mednick, and W. R. Grise, Phys. Rev. B **26**, 6379 (1982).
[40] D. M. Bylander, L. Kleinman, and K. Mednick, Phys. Rev. B **25**, 1090 (1982).
[41] W. R. L. Lambrecht, N. E. Christensen, and P. Blöchl, Phys. Rev. B **36**, 2493 (1987).
[42] O. Bisi and C. Calandra, J. Phys. C **14**, 5479 (1981).
[43] X. Jian-hua and X. Yong-nian, Solid State Commun. **55**, 891 (1985).
[44] J. M. Van Ruitenbeck, W. Joss, R. Pauthenet, O. Thomas, J. P. Senateur, and R. Madar, Phys. Rev. B **35**, 7936 (1987).
[45] R. D. Frampton, E. A. Irene, and F. M. d'Heurle, J. Appl. Phys. **59**, 978 (1986).
[46] D. W. Lynch, R. Rosei, and J. H. Weaver, Solid State Commun. **9**, 2195 (1971).
[47] J. M. Pimbley and W. Katz, Appl. Phys. Lett. **42**, 984 (1983).
[48] J. H. Weaver, D. W. Lynch, and C. G. Olson, Phys. Rev. B **10**, 501 (1974).
[49] D. E. Aspnes, in *Handbook of Optical Constants of Solids*, edited by E. D. Palik (Academic, Orlando, 1985), Chap.5.
[50] H. R. Philipp, in *Handbook of Optical Constants of Solids*, edited by E. D. Palik (Academic, Orlando, 1985), p.749.
[51] F. Nava (private communication).
[52] M. Gurvitch, A. F. J. Levy, R. T. Tung, and S. Nakashara, Mater. Res. Symp. Proc. **91**, 457 (1987).
[53] C.Vignier, thésis, Université de Aix-Marseille, 1987.

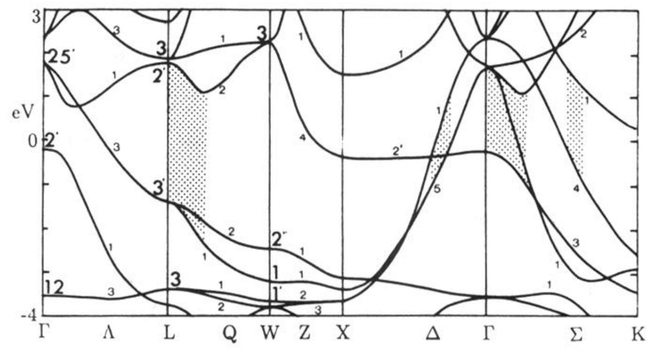


FIG. 9. Energy bands near the Fermi level for $NiSi_2$ (from Bylander *et al.*, Ref. 39). The dashed areas represent allowed transitions determining structures in the joint density of states.